JOURNAL OF AIRCRAFT
Vol. 33, No. 5, September–October 1996

Performance of a Propeller Embedded in the Flowfield of a Wing

Rosario M. Ardito Marretta*
University of Palermo, 90128 Palermo, Italy

A technique based on the method of free wake analysis (FWA) was developed to analyze the interference between an aircraft propeller and a wing and, specifically, to compute the influence of the wing aerodynamic field on the propeller performance. For an isolated propeller and wing, the models employed were based on the FWA and implemented Prandtl theory, respectively. The effects on performance were related to the wing angle of attack and to the variation of wing circulation and its effect on the induced velocity at the propeller disk. The aim of this article is the determination of the propeller performance as related to the change of the propeller inflow because of the presence of the wing and the resulting change of the performance. The robustness of the method was tested against the available experimental data obtained on a model scale of an isolated propeller. The results, when wing and propeller are coupled, show the variation of thrust, power, and efficiency with the previously mentioned parameters and blade pitch.

Nomenclature

A = tip vortex contraction coefficient, Eq. (2)
a = experimentally determined constant, Eq. (2)
B = number of blades
C_L = wing lift coefficient
C_P = power coefficient, $P/\rho n^3 D^5$
C_T = thrust coefficient, $T/\rho n^2 D^4$
H = induced velocity parameter, Eq. (8)
J = propeller advance ratio, U_∞/nD
K_1, K_2 = tip vortex translation coefficients, Eqs. (3) and (4)
n = blade rotational frequency, rps
$OXYZ$ = fixed coordinate system, Fig. 1
P = power of the propeller, $2\pi nQ$, W
Q = propeller torque, Nm
q = velocity induced by the wing, m/s
R = radius of propeller, m
R_0 = radius of propeller hub, m
r_t = radial contraction of the tip vortex in the propeller wake, m
r_v = radial contraction of a vortex from the point ξ on the blade, m
T = thrust of the propeller, N
U_∞ = freestream velocity, m/s
u, v, w = velocity components, m/s
V_{il} = velocity induced by free vortices, m/s
x_t = axial convection of propeller tip vortex, m
x_v = axial convection of any vortex of the propeller wake, m
α = angle of attack, deg
β_0 = propeller blade angle, deg
Γ = circulation, m^2/s
ΔC_P = oscillation of power coefficient
ΔC_T = oscillation of thrust coefficient
η = efficiency of the propeller
θ = angular increment of blade rotation, deg
ξ = fraction of blade radius, r/R
ψ = azimuth coordinate in the propeller wake, deg
Ω = rotational speed, rad/s

Received Nov. 10, 1995; revision received May 17, 1996; accepted for publication May 17, 1996.

*Research Engineer, Department of Mechanics and Aeronautics, Viale delle Scienze.

Introduction

FOR studying the complex flows arising from the aerodynamic interaction between a propeller in tractor configuration and the wing on which it is mounted, the aerodynamic field near the wake of the propeller has been analyzed. Some efforts are to be tied, from the point of view of a numerical approach to the solutions of the governing integro-differential equations. The free wake analysis method (FWA), as demonstrated by new experimental results, is successful in numerically determining the wing-propeller interference. The behavior and the mechanism of the interaction between wing and propeller has been described by Witkowski et al.,[1] by assuming that the flowfield is inviscid and quasisteady behind the propeller, and by Cho and Williams[2] and Rottgermann and Wagner,[3] who focused the problem on frequencies dominant in unsteady flows. The isolated propeller was analyzed by Kinnas and Hsin[4] using the boundary element method (BEM). Only when the blade tip speed is low enough so as not to cause compressibility effects, does the comparison of their large quantity of results show that the conclusions obtained by using the quasisteady model are similar to those of the more complex unsteady one. The numerical procedure usually involves a discretization into a large number of panels for both the wing and the blade, whereas here a single vortex line may be sufficient to model each blade of the propeller.

To focus attention on the influence of the finite wing aerodynamic field on the propeller performance, in terms of thrust, torque, and efficiency, no effects on aircraft dynamics will be considered as well as the distortion of the inflow near the blade roots and its interference with the hub. Following Favier et al.[5–7] and Marretta,[8] the isolated propeller and wing in an asymptotic stream are considered first and the FWA method is then used for finding the numerical results that form the basis for achieving a proper numerical simulation of the mutual influence of the wing–propeller on the performance of the aircraft. By representing the wake and propeller blades by lifting lines, more detailed results become available for the flow past the propeller. Moreover, to avoid loss in precision, instead of the classical Prandtl scheme, the theory from Pistolesi–Weissinger,[9] in which the bound vortex is placed at the wing quarter-chord line and the velocity tangency condition to the surface is imposed at the three-quarter chord line, is employed here.[10]

By developing a complete numerical procedure, this may be applied to both aerodynamic fields successively.[1,2,11] Then the

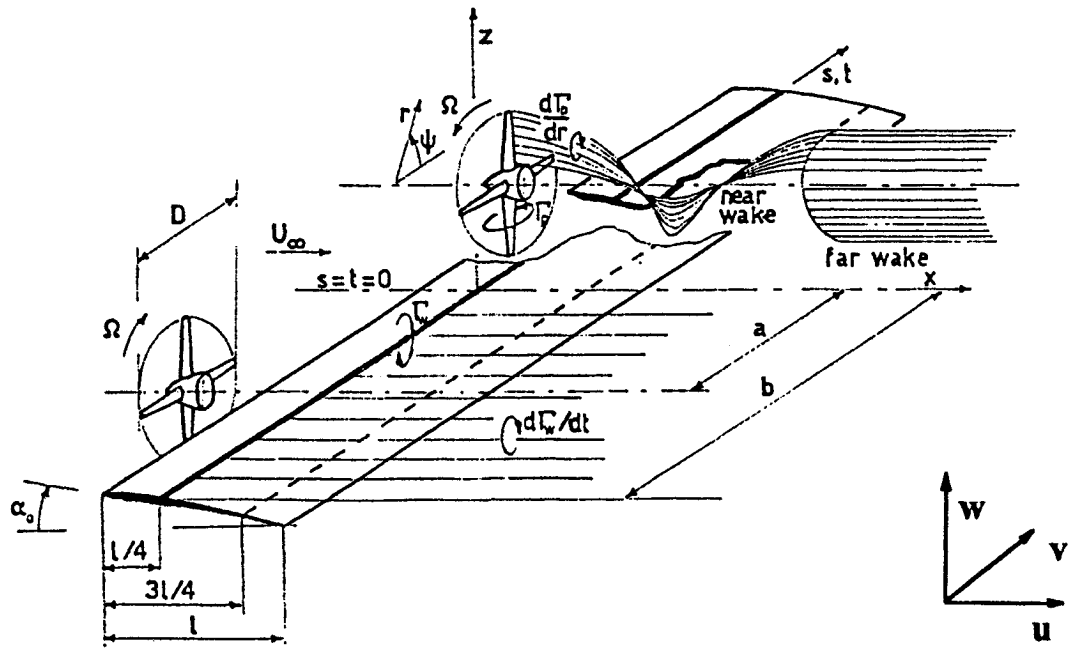

Fig. 1 Configuration of the wing-propeller geometry and wake.

variations of the performance characteristics of the tractor propeller are developed in terms of the wing angle of attack, the variation of circulation, and the induced velocity field near the leading edge, or more accurately, near the propeller disk area. In fact, that region shows change in the asymptotic condition of the flow, and therefore, the propeller operating condition. The results demonstrate that variations in thrust, torque or power, and efficiency are now larger as α and β_0 increase.

Mathematical Models

To find the solution to this aerodynamic problem it is necessary for a useful result to analyze and model the wake past the propeller blades. In this article the FWA approach is first applied to an isolated propeller. This iterative method is based on a convergence criterion imposed on the sheet of vortices leaving each blade to form the propeller wake and are made up of all the vortex lines starting from the points on the blade.[5-7]

Following Favier et al.,[5] r_t and x_t are put in relation to ψ and remain valid in the region near the propeller disk, the so-called near wake; outside a value ψ_s (far-wake), the region of flow becomes unstable (see Fig. 1). Through Eq. (1) the value of ψ_s is related to J, β_0, and B:

$$(\psi_s - \psi_B)/B \cdot \psi_B = 0.25[8.5 - \beta_0/10 - J \cdot (J + 2)] \quad (1)$$

where ψ_B is the angle between each blade, $=360/B$.

On the other hand for tip vortex paths one obtains:

$$r_t/R = A + (1 - a) \cdot e^{-\psi/B} \quad \text{for} \quad 0 \le \psi \le \psi_s \quad (2)$$

$$x_t/R = K_1 \cdot (\psi/\psi_B - 1) \quad \text{for} \quad 0 \le \psi \le \psi_B \quad (3)$$

$$x_t/R = K_1 + K_2 \cdot (\psi/\psi_B - 1) \quad \text{for} \quad \psi_B \le \psi \le \psi_s \quad (4)$$

where A, K_1, and K_2 are related to β_0 and J. By considering the relationship between r_v and the tip vortex contraction, we have

$$r_v/R = \xi \cdot r_t(\psi) \quad \text{for} \quad 0 \le \psi \le \psi_s \quad (5)$$

and for x_v one obtains

$$x_v/R = H(r, 0) \cdot \psi \quad \text{for} \quad 0 \le \psi \le \psi_B \quad (6)$$

$$x_v/R = H(r, 0) \cdot \psi_B + H(r, \psi_B) \cdot (\psi - \psi_B) \quad \text{for} \quad \psi_B \le \psi \le \psi_s \quad (7)$$

where the functions $H(r, 0)$ and $H(r, \psi)$ depend on the coordinates of the vortex filament (ψ, ψ_B).

The velocities u, v, and w induced by the wing and wake at any point on the blade may be obtained by relating C_L to the wing and wake vortex strengths and by using the Kutta–Joukowski theorem. Then H may be found as a function of u, v, w, and ψ:

$$H(u, v, w, \psi) = (\pi/180) \cdot (V_0 + u)/[\Omega + (v \cdot \cos\psi - w \cdot \sin\psi)/r] \quad (8)$$

It should be noted that the induced velocity w is given, different in sign, as it may be seen later, by the half-Hilbert term in Eq. (15). Through Biot–Savart's law, applied to the blade circulation $\Gamma(\xi)$ and the trailing wake vortices, one obtains the induced velocity at any point in the wake as follows:

$$V = \frac{1}{4\pi} \cdot \int_{R_0}^{R} \Gamma(\xi) \cdot \frac{d\boldsymbol{l} \wedge \boldsymbol{r}}{|\boldsymbol{r}|^3} + \frac{1}{4\pi} \cdot \int_{R_0}^{R} \left[\frac{-d\Gamma(\xi)}{d\xi} \cdot \int_{L(\xi)} \frac{d\boldsymbol{l} \wedge \boldsymbol{r}}{|\boldsymbol{r}|^3} \right] \cdot d\xi \quad (9)$$

In Eq. (9), $\boldsymbol{r}$ represents the position vector of a space point P with respect to the vortex coordinate system, $L(\xi)$ is the vortex filament leaving the point ξ of the blade, and $d\boldsymbol{l}$ is the vector parallel to the direction of the bound vortex in the first integral, and to the trailing vortex filaments in the second one.

By noting that the bound vortices have no influence and then $d\boldsymbol{l} \wedge \boldsymbol{r}$ vanishes in the near-wake regions, and having determined Γ from Eq. (9), the velocity at the point P of the sheet vortices may be written as a superposition, on each blade, of each integral:

$$\boldsymbol{V}_{ia}(P) = \frac{1}{4\pi} \cdot \sum_{p=1}^{MP} \int_{R_0}^{R} \Gamma(\xi) \cdot \frac{\boldsymbol{\tau}_p \wedge \boldsymbol{r}_p}{|\boldsymbol{r}|^3} \cdot d\xi \quad (10)$$

therefore, V_{il} induced by the free vortices at P may be written in the form of

$$\boldsymbol{V}_{il}(P) = \frac{1}{4\pi} \cdot \int_{R_0}^{R} \frac{d\Gamma(\xi)}{d\xi} \cdot \boldsymbol{G}(P, \xi) \cdot d\xi \quad (11)$$

where the coefficients of influence $G(P, \xi)$ are expressed as follows:

$$G(P, \xi) = -\int_{Lp(\xi)} \sum_{p=1}^{MP} \frac{\tau_p \wedge r_p}{|r_p|^3} \cdot dl \tag{12}$$

As regards the far-wake regions, the influence of an elementary ring vortex C on the induced velocity is given by the following integral expression:

$$\int_C \frac{dl \wedge r}{|r|^3} \tag{13}$$

which is solved numerically.

Numerical Simulation

To obtain the parameters of the propeller performance, we assign the number of blades as well as their dimensional and design characteristics β_0, the geometric twist, the diameters R and R_0, the freestream velocity, and Ω. Based on the previous literature concerning numerical results and experimental data,[5-8] the aerodynamic characteristics of the blade airfoil sections can be introduced.

Specifically, a four-bladed propeller mounted on a Partenavia AP 68TP-600 Aviator and having hub and overall diameters of 0.4 and 2.0 m, respectively, is considered. The range of values of J is 0.2–0.8, and the mean blade pitch setting varies from 23 to 32.5 deg. The distance between the propeller axis and wing midspan and the distance between the propeller disk and the wing leading edge were 2 and 0.2 m, respectively. In this article the blades have constant NACA 64A408 airfoil sections.

The previous nonlinear system is solved by the iterative Newton–Raphson method; the pitch of the helical vortex filaments is equal to the translation per revolution, the calculated velocity field becomes tangent at the points of each vortex line and the sheet vortex deformation becomes negligible. The output of the model gives the velocity field, circulation distribution, wake geometry, as well as the performance characteristics of the propeller, namely C_T, C_P, and η (see Figs. 2, 3, and 4). The purpose of the present investigation is to address some points previously raised[8,11] and to show the effects of the presence of the wing behind the propeller on the coefficients C_T, C_P, and η. The wing circulation also induces a velocity field on the wake of the propeller giving, in effect, a change in the direction of the wake and J. Since the wing circulation and the induced velocities are to be related to the angle of attack, the performance of the propeller is determined as a function of α from 2 to 12 deg.

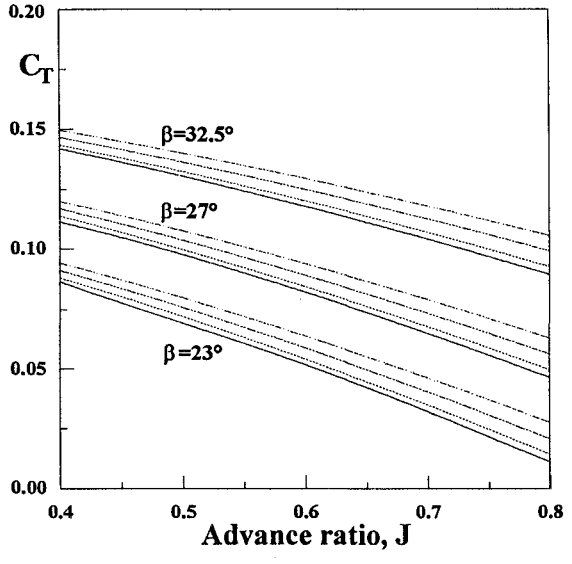

Fig. 2 Propeller thrust coefficient: ——, isolated; · · ·, α = 2 deg; —··, α = 6 deg; and —·, α = 12 deg.

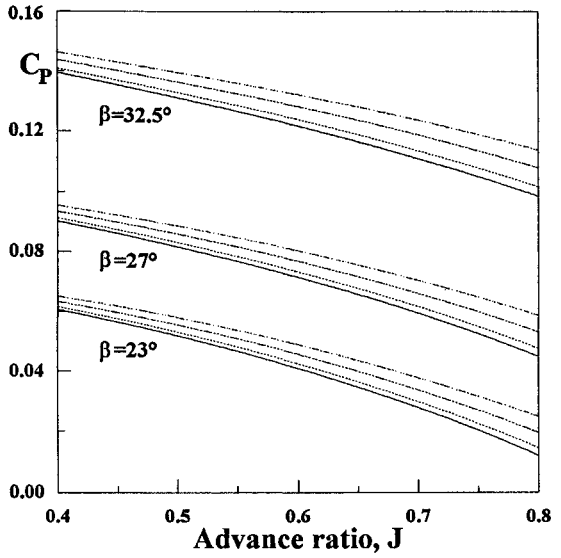

Fig. 3 Propeller power coefficient: ——, isolated; · · ·, α = 2 deg; —··, α = 6 deg; and —·, α = 12 deg.

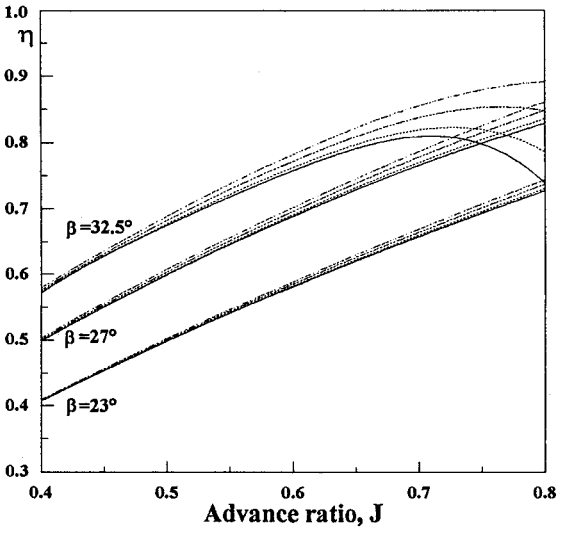

Fig. 4 Propeller efficiency: ——, isolated; · · ·, α = 2 deg; —··, α = 6 deg; and —·, α = 12 deg.

To avoid the approximation of the classical Prandtl horseshoe vortical model for the wing, the form of the theory from Pistolesi–Weissinger,[6] in which the bound vortex is placed on the wing quarter-chord line and the tangency condition to the surface is enforced at the three-quarter chord line, is used here. By assuming a straight wing geometry and making the hypotheses of steady flow and negligible effects of vortex roll-up, and, regarding the wake and the wing to be coplanar, one obtains an integro-differential equation that contains the transform of the circulation, with its relative boundary condition $\Gamma = 0$ at wingtips. By assuming the wing can be described by a lifting line whose equation is

$$z_{1/4} = 0 \tag{14a}$$

one obtains Eq. (14b) for the three-quarter chord line:

$$z_{3/4} - z_{1/4} = c_0/2 \tag{14b}$$

in which c_0 represents the centerline chord.

By using linear approximation, the system of wake vortices is represented by a set of free vortices lying in the wing plane and parallel to the freestream and leaving three-quarter chord line downstream. By making use of the extension of Prandtl's lifting line theory from Weissinger, we replace the wing by a bound vortex placed at the points of the quarter-chord line. The vortex circulation $\Gamma_w(s)$ varies along the nondimensional wingspan s, whose tips are at $s = \pm 1$, and is of magnitude such that its own induced velocity added to that given by the trailing vortices results in the flow velocity being tangent to the wing three-quarter chord line. This method was applied[10] to a complex but isolated wing plane geometry, but has been described in detail for an unswept but not isolated rectangular wing. By integrating along the lifting line and by collecting the two previously mentioned contributions, one obtains the induced velocity. Once the Pistolesi–Weissinger condition between induced velocity and angle of attack has been imposed, and by normalizing the induced velocity and geometry parameters by U_∞ and the semispan x_0, respectively, the integro-differential equation is obtained:

$$2\cdot\alpha_0(s) = \frac{1}{\pi}\cdot\int_{-1}^{1}\frac{d\Gamma w}{dt}\cdot\frac{dt}{s-t} + \frac{1}{\pi}\cdot\int_{-1}^{1} T(s,t)\cdot\Gamma w(t)\cdot dt \qquad -1 \le s \le 1 \tag{15}$$

where $T(s, t)$ is given by

$$T(s,t) = 2/\sqrt{c^2 + 4\cdot(s-t)^2}\left[1 + \sqrt{c^2 + 4\cdot(s-t)^2}\right] \tag{16}$$

being c the (constant) wing chord, and s the spanwise coordinate along the lifting line. The tip boundary condition for the circulation is $\Gamma(-1) = \Gamma(1) = 0$.

Suitable mathematical procedures[11,12] applied to Eq. (15) lead to a numerical solution for the circulation that can be expressed as follows:

$$\Gamma w(t) = (1 - t^2)^{1/2}\cdot\sum_{j=1}^{N}\xi_j\cdot\frac{U_N(t)}{(t - t_j)\cdot U'_N(t_j)} \tag{17}$$

where $U_N(t)$ ($N = 1, 2, \ldots$) are the Chebyshev polynomials of the second kind with t_j their zeroes.

Through the following relationships one obtains the collocation points s_k and t_j:

$$s_k = \cos\{k\cdot[\pi/(n+1)]\} \qquad t_j = \cos\{j\cdot[\pi/(n+1)]\} \tag{18}$$

Input wing data consist of the (constant) chord equal to 1.5 m, AR = 8, wingspan 12 m, and the number of collocation points at which the values of circulation and the induced velocities will be calculated. Like the propeller, the wing has a NACA 64A408 airfoil and negligible dihedral angle. As regards the output data, these were input to the propeller to determine the influence of the wing on the coefficients C_T, C_P, and η, now calculated corresponding to the altered J. Assuming a fixed coordinate system X, Y, and Z, and taking the X axis along the direction of the wing chord, Y along the wingspan, and Z directed up, the general representation for the induced velocities field caused by the trailing vortices $d\Gamma$ leaving the finite wingspan is given by[8,12]:

$$q_{tot} = \left(\frac{Z,\ 0,\ -X}{Z^2 + X^2}\right)\cdot\frac{1}{4\pi}\cdot\int_{-b}^{b}\left(\frac{Y+\mu}{\Theta} - \frac{Y-\mu}{T}\right)\cdot\frac{d\Gamma}{d\mu}\,d\mu + \frac{1}{4\pi}\cdot\int_{-b}^{b}\left[\frac{0,\ Z,\ -(Y+\mu)}{\Xi}\right]\cdot\left(1 + \frac{X}{\Theta}\right)\cdot\frac{d\Gamma}{d\mu}\,d\mu - \frac{1}{4\pi}\cdot\int_{-b}^{b}\left(\frac{0,\ Z,\ \mu - Y}{E}\right)\cdot\left(1 + \frac{X}{\Theta}\right)\cdot\frac{d\Gamma}{d\mu}\,d\mu \tag{19}$$

where

$$\Theta = \sqrt{X^2 + (Y+\mu)^2 + Z^2}$$
$$T = \sqrt{X^2 + (Y-\mu)^2 + Z^2}, \qquad \Xi = Z^2 + (Y+\mu)^2 \tag{20}$$
$$E = Z^2 + (\mu - Y)^2$$

$\Gamma(\mu)$ is the wing bound circulation and $\mu = \cos(k\pi/k + 1)$ is the nondimensional coordinate along the wingspan. Having reduced the integration path and integrating by parts Eq. (19), and by taking into account the boundary conditions, one obtains, through suitable limit procedure, an integral equation in which only the circulation and not its derivative is present:

$$q_{tot} = \frac{\Gamma(\mu)(\mu_2 - \mu_1)}{4\pi}\cdot\int_{-b}^{b}\frac{\partial}{\partial\mu}\left(\left\{\frac{Z,\ 0,\ -X}{Z^2 + X^2}\cdot\frac{(Y-\mu)}{T} + \left[\frac{0,\ Z,\ (Y-\mu)}{Z^2 - (Y+\mu)^2}\right]\left(1 + \frac{X}{T}\right)\right\}\right)d\mu \tag{20a}$$

Through Gaussian quadrature the components of velocity can be finally determined where x, y, and z are obtained from

$$x = -a - l/4, \qquad y = d + r\cdot\cos\vartheta, \qquad z = r\cdot\sin\vartheta \tag{21}$$

where a and $l/4$ represent, respectively, the position of the propeller disk plane and the quarter-chord with respect to the wing leading edge, d the distance between the propeller rotational axis and $Y = 0$, r a point on the blade radius, and θ the instantaneous blade azimuth. The previous fixed coordinate system X, Y, and Z does not take into account the instantaneous position of the blade. Therefore, the local velocity components have been projected in a rotating coordinate system placed at a point P of the blade in such a way that q_x becomes the reduced axial velocity component normal to the propeller disk plane, q_y and q_z the reduced radial and tangential components, respectively. Having found these components from Eq. (19), and taking into account the radial deformation of the wake, though not large, one obtains the new coefficients C_T, C_P, and η. As previously described[8] for a two-bladed propeller, C_T, C_P, and η are related to J and θ (noting that unlike the two-bladed case, with four blades the positions at 0 deg for two blades implies a position of 90 deg for the others and only 45 deg

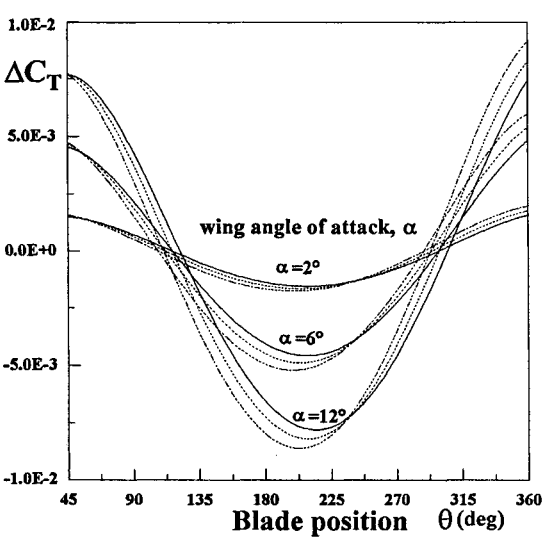

Fig. 5 Oscillation of the thrust coefficient for $\gamma = 0.4$: ——, $\beta_0 = 23$ deg; ···, $\beta_0 = 27$ deg; and ---, $\beta_0 = 32$ deg.

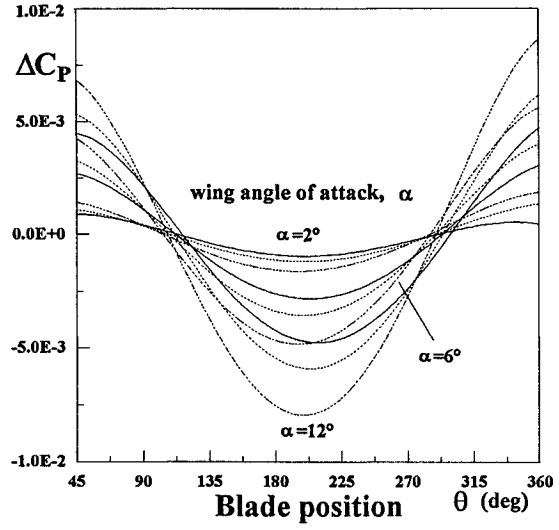

Fig. 6 Oscillation of the power coefficient for γ = 0.4: ——, β_0 = 23 deg; ···, β_0 = 27 deg; and ---, β_0 = 32 deg.

has been considered at first), the angle of attack 2, 6, and 12 deg and the mean blade pitch 23, 27, and 32.5 deg.

Figures 2–4 show the coefficients C_T, C_P, and η both for the isolated and installed propeller. Figures 5 and 6 contain the calculated behavior of the thrust and power variation, ΔC_T and ΔC_P, as a function of θ, α, and β_0.

The amplitude of these oscillations being defined by the values of ΔC_T, and ΔC_P obtained for each instantaneous position of blade θ by the difference between $C_{T\max}$ and $C_{T(\theta)}$, once α and β_0 are assigned with and without interference between wing and propeller.

Results and Discussion

From Figs. 2–4, when β_0 = 32.5 deg and α = 12 deg, the thrust coefficient C_T increases about 5% from 0.14191 to 0.14959. Because of the interference of the wing on the propeller, respectively, likewise C_P increases by 4.9% from 0.13948 to 0.14627 and η increases $\frac{1}{2}$% from 0.40753 to 0.40962. Because of the change in the velocity field, the free-stream axial velocity decreases and therefore so does J, giving an increase of the coefficients C_T, C_P, and η. Figures 2–4 show again C_T, C_P, and η for a set of values of α. Once J is fixed, the most significant variations of C_T and C_P are related to the increase in β_0, but these are less significant than the effects of increasing α. The thrust is more sensitive to the change of blade pitch than angle of attack for the same flight conditions and for the same blade angular position. This is also true for the power coefficient and efficiency, although a significant variation of efficiency resulting from α was calculated for β_0 = 32.5 deg.

Figures 5 and 6 show the variations of C_T and C_P, with blade position for a given advance ratio, angle of attack, and blade pitch angle. Once β_0, J, and α are given, the amplitude of thrust and power is the difference between the values of C_T and C_P, with and without interference, for a given θ. The amplitude of C_T decreases between θ = 45–225 deg and increases between θ = 225–0 deg. The same conclusions may be deduced from the point of view of power; the efficiency curves are omitted because their difference in values is negligible. The values of C_T are not perfectly periodic with θ because the wing wake is not symmetrical behind the propeller. From Figs. 5 and 6 it can be seen that the largest values of ΔC_T and ΔC_P are associated with increasing α and β_0. It may be worth noting that, even though the largest variations of thrust and power are associated with the largest α and β_0, these occur within a relative range of θ [120–240 deg]; however, at lower values of α and β_0 these persist for a longer period θ [60–360 deg]. To explain this real oscillation in thrust one has to look at the effect of the position of the blade. For a given α and β_0, when the two blades are in a vertical position (90 ± 15 deg) in contrast to the horizontal position, the wing-induced velocities that are changing not only along the wingspan, but also orthogonal to the wing leading edge, will additionally influence the asymptotic condition of flow (it may be suitable to underline the raising of induced longitudinal stream along the wingspan). It should also be noted that for two values of θ, 112 deg and 112 deg + π, the variation in C_T and C_P vanishes (the set of curves merge).

Conclusions

A numerical methodology based on and according to previous results has been presented for solving the aerodynamic problem of the characteristics of a propeller mounted in front of a wing, for a wide range of design and flight parameters. The approach presented shows a numerical evaluation of the interference of the induced velocity field caused by the presence of the wing and its effect on a tractor propeller and its performance.

Some improvement of the method may be obtained by taking into account the conditions of flow near the blade root. This region, in fact, shows the most significant disagreements between the experimental and theoretical results.

References

[1]Witkowski, D., Lee, A., and Sullivan, J., "Aerodynamic Interactions Between Propellers and Wings," *Journal of Aircraft*, Vol. 26, No. 9, 1989, pp. 829–836.

[2]Cho, J., and Williams, M. H., "Propeller-Wing Interaction Using a Frequency Domain Panel Method," *Journal of Aircraft*, Vol. 27, No. 3, 1990, pp. 196–203.

[3]Rottgermann, A., and Wagner, S., "Compressible Potential Flow Around a Helicopter Rotor," *Proceedings of the Symposium ICES-IABEM'95* (Kona, HI), Springer–Verlag, Vol. 2, 1995, pp. 2915–2920.

[4]Kinnas, A. S., and Hsin, C. Y., "Boundary Element Method for the Analysis of the Unsteady Flow Around Extreme Propeller Geometries," *AIAA Journal*, Vol. 30, No. 3, 1992, pp. 688–696.

[5]Favier, D., Ettaouil, A., and Maresca, C., "Numerical and Experimental Investigation of Isolated Propeller Wakes in Axial Flight," *Journal of Aircraft*, Vol. 26, No. 9, 1989, pp. 837–846.

[6]Favier, D., and Maresca, C., "Etude du Sillage 3D d'une Hélice Aérienne Quadripale," *AGARD FDP on Aerodynamics and Acoustics of Propellers*, CP-366, AGARD, Oct. 1984 (Paper 15).

[7]Favier, D., Nsi Mba, M., Barbi, C., and Maresca, C., "A Free-Wake Analysis for Hovering Rotors and Advancing Propellers," *Proceedings of the 11th European Rotorcraft Forum*, Paper 21, London, 1985, pp. 493–511.

[8]Marretta, M. R., and Lombardo, G., "Coefficienti di Trazione, di Coppia e Rendimento dell'Elica in Presenza del Campo Aerodinamico di un'Ala Finita," *Aerotecnica—Missili e Spazio*, Vol. 73, Nos. 1, 2, 1994, pp. 31–41.

[9]Weissinger, J., "Uber die Auftriebverteilung von Pfeilflugen," Forschungsberichte der Berliner Zentrale für wissenschaftliches Berichtswesen 1553, Berlin-Adlershof, 1942.

[10]Prossdorf, S., and Tordella, D., "On an Extension of Prandtl's Lifting Line Theory to Curved Wings," *Impact of Computing in Science and Engineering*, Vol. 3, Jan. 1991, pp. 192–212.

[11]Chiocchia, G., and Pignataro, S., "On the Induced Drag Reduction Due to the Propeller-Wing Interaction," *The Aeronautical Journal of the Royal Aeronautical Society*, Vol. 99, No. 988, 1995, pp. 328–336.

[12]Robinson, A., and Laurmann, J. A., "Wing Theory," *Cambridge Aeronautical Series*, 1st ed., Vol. 2, Cambridge Univ. Press, Cambridge, England, UK, 1956, pp. 28–36.